

Spatial Configuration and Three-Dimensional Conformation Directed Design, Synthesis, Antiviral Activity, and Structure–Activity Relationships of Phenanthroindolizidine Analogues

Bo Su, Chunlong Cai, Meng Deng, and Qingmin Wang*

State Key Laboratory of Elemento-Organic Chemistry, Research Institute of Elemento-Organic Chemistry, Collaborative Innovation Center of Chemical Science and Engineering (Tianjin), Nankai University, Tianjin 300071, People's Republic of China

Supporting Information

ABSTRACT: Our recent investigation on the antiviral activities against tobacco mosaic virus (TMV) of phenanthroindolizidine alkaloid analogues preliminarily revealed that the basic skeleton and substitution pattern at the C13a position of the molecule, which are closely related to the spatial arrangement of the molecule, have great effects on the biological activity. To further study the in-depth influence of spatial configuration and three-dimensional (3D) conformation of the molecules on their anti-TMV activities and related structure–activity relationship (SAR), a series of D-ring opened derivatives **3**, **4**, **5a–5j**, **6**, and **7**, chiral 13a- and/or 14-substituted phenanthroindolizidine analogues **10–12** and **18–20**, and their enantiomers **ent-10–ent-12** and **ent-18–ent-20** were synthesized and evaluated for their anti-TMV activities. Bioassay results showed that most of the chiral phenanthroindolizidines displayed good to excellent *in vivo* anti-TMV activity. Among these compounds, **ent-11** showed more potent activity than Ningnanmycin (one of the most successful commercial antiviral agents), thus emerging as a potential inhibitor of the plant virus. Further SARs were also discussed for the first time under the chiral scenario, demonstrating that both spatial configuration and 3D conformation of the molecules are crucial for keeping high anti-TMV activity.

KEYWORDS: phenanthroindolizidine alkaloid, antiviral activity, tobacco mosaic virus, structure–activity relationship, anti-TMV

INTRODUCTION

Tobacco mosaic virus (TMV), the first virus that had ever been discovered and purified, has been known for over 1 century, dating back to Benjerinck's description of mosaic disease of tobacco as a *contagium vivum fluidum* and the modern usage of the term "virus".¹ It is known that more than 125 individual species of 9 plant families (such as tobacco, pepper, cucumber, tomato, many ornamental flowers, etc.) can be infected by TMV.² TMV is the most persistent plant virus known, which can survive in dry plant debris for as long as 100 years; therefore, it is very difficult to control once plants have been infected. TMV causes serious damage worldwide, and the economic loss each year is up to U.S. \$100 million.³

Ningnanmycin (Figure 1), displaying 56.0% inhibitory effect at 500 $\mu\text{g mL}^{-1}$, is almost the most effective commercially available anti-plant virus agent. Ribavirin (Figure 1), another plant virus inhibitor, is widely used, and its inhibitory effect is always less than 50% at 500 $\mu\text{g mL}^{-1}$. Because TMV causes large economic loss every year and commercial plant virucides could always not show a satisfactory inhibitory effect (usually 30–60%), the development of novel and more potent antiplant virus agents is very appealing. Consequently, as a result of their known antiviral activities, some chemicals, such as pyrazole derivatives,⁴ nucleotides,⁵ α -aminophosphonate derivatives,⁶ 3-acetonyl-3-hydroxyindole,⁷ triazolyl compounds,⁸ oxidized polyamines,⁹ and substituted phenylureas,¹⁰ have been investigated extensively. However, few of them have been successfully developed and applied in agriculture.

In comparison to synthetic chemicals, natural-product-based TMV inhibitors are less toxic to the environment, easier to

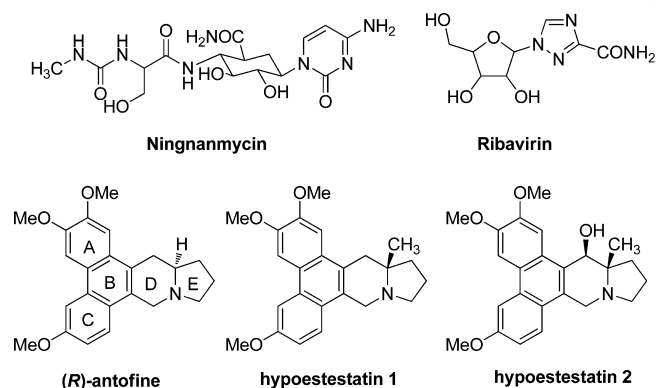


Figure 1. Chemical structures of Ningnanmycin, ribavirin, and representative phenanthroindolizidine alkaloids.

decompose, and specific to a target species, have a unique mode of action, etc.^{11,12} Phenanthroindolizidine alkaloids are a small class of pentacyclic natural products,¹³ which possess a range of biological activities, such as anticancer, anti-inflammatory, antiamoebic, antilupus effects, etc.^{14–18} Ten years ago, our group initiated a project aiming at seeking natural biologically active compounds as alternatives to synthetic chemicals and first found that the alcohol extract of *Cynanchum komarovii* showed a moderate inhibitory effect against TMV.¹⁹ (R)-

Received: December 26, 2015

Revised: February 17, 2016

Accepted: February 28, 2016

Published: February 28, 2016



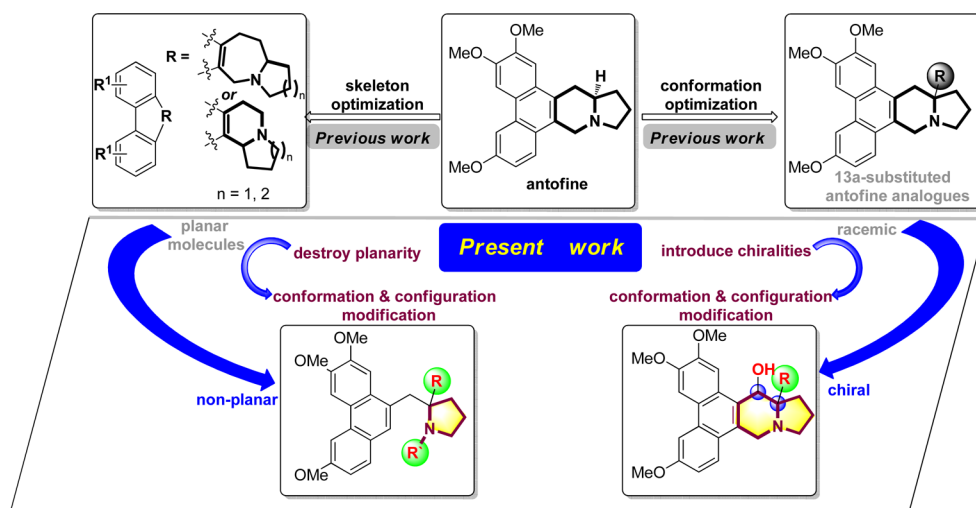


Figure 2. Design of the targeted molecules based on spatial configuration and 3D conformation and modification.

Antofine was then proven to be the main active compound (Figure 1). Mechanism studies against TMV indicated that, as a result of the favorable interaction with the origin of TMV RNA (oriRNA), antofine exhibits its antiviral activity by binding to oriRNA and interfering with virus assembly initiation.²⁰ Distinguished from the common 13a-H phenanthroindolizidine alkaloids, hypoestestatins 1 (Figure 1) possesses a methyl group at the C13a position.²¹ Since its discovery in 1984, several other 13a-methyl-phenanthroindolizidine alkaloids were subsequently reported.^{22,23} However, in comparison to their 13a-H counterparts, these structurally novel 13a-substituted antofine analogues were rarely investigated.

Although a structure–activity relationship (SAR) study on 13a-H antofine analogues has been investigated extensively,^{24–28} the previous research was only limited to substitution effects on the phenanthryl ring and precursors en route to these natural products or analogues, mainly as a result of the underdevelopment of the synthetic methodology about these alkaloids. However, a simple modification of the phenanthryl ring of the pentacyclic structure of phenanthroindolizidine alkaloid can only adjust its electronic or steric property but does not have much influence on its spatial configuration and three-dimensional (3D) conformation. In fact, the latter factors play a more important role in adjusting the delicate interaction between the specific molecule and the target and, thus, are more essential for the investigation of in-depth SARs. Toward this goal, we initially designed and synthesized two types of structurally novel antofine analogues, which changed the size of the D ring or the arrangement of D/E rings from the mother pentacyclic phenanthroindolizidine significantly. Bioassay results demonstrated for the first time that the original spatial arrangement of phenanthroindolizidines was not optimal for these alkaloids to keep high activities.²⁹ Inspired by the unique structure of the 13a-methyl-phenanthroindolizidine alkaloid hypoestestatins 1 and 2 (Figure 1), we then introduced a series of functional groups at the bridgehead of the D/E ring of phenanthroindolizidine alkaloids, largely varying their 3D conformation from their 13a-H counterparts. Antivirus activity results showed that some of the C-13a-substituted derivatives were indeed much more potent than antofine.³⁰ Therefore, these results demonstrated that further studies based on this line was in demand.

To further systematically investigate the in-depth influence of spatial configuration and 3D conformation of phenanthroindolizidine alkaloids on the antiviral activities (Figure 2), a series of D-ring opened 13a-substituted alkaloid analogues and chiral 13a- and/or 14-substituted alkaloids were designed, synthesized, and evaluated for their antiviral activity against TMV. The SAR study of these compounds was also discussed for the first time under the chiral scenario.

MATERIALS AND METHODS

Chemicals. Reagents, such as proline, di-*tert*-butyl dicarbonate, trifluoroacetyl chloride, acetyl chloride, trimethylacetyl chloride, benzoyl chloride, ethyl carbonochloridate, benzyl carbonochloridate, benzyl carbonochloridate, 4-methylbenzene-1-sulfonyl chloride, methyl iodide, benzyl bromide, thionyl chloride, bromine, triethylamine, and potassium carbonate, were purchased from Tianjin Reagents 6th Company and used directly without further purification. Sodium, *tert*-butyllithium, lithium diisopropylamide, lithium aluminum hydride, and lithium triethylborohydride were purchased from Alfa Aesar and used as received. All anhydrous solvents, such as tetrahydrofuran (THF), dichloromethane (DCM), and dimethylformamide (DMF), purchased from Tianjin Reagents 6th Company, were dried and purified according to standard techniques just before use. Other solvents, such as methanol, ethanol, petroleum ether, and ethyl acetate, were purchased from Tianjin Reagents 6th Company and used directly without further purification.

Instruments. High-resolution mass spectra (HRMS) were recorded on Fourier transform ion cyclotron resonance mass spectrometry (FT-ICR MS, Ionspec, 7.0 T). Melting points were determined on an X-4 binocular microscope melting point apparatus and were uncorrected.

1-*tert*-Butyl-2-methyl-2-((3,6,7-trimethoxyphenanthren-9-yl)methyl)pyrrolidine-1,2-dicarboxylate (3). To a solution of *i*-Pr₂NH (0.9 g, 9.0 mmol) in THF (10 mL) was added *n*-BuLi (4.3 mL, 2.2 M in hexane, 9.5 mL) dropwise at -78°C under Ar. After 10 min, a solution of compound 2 (2.06 g, 9.0 mmol) in THF (10 mL) was added dropwise. The reaction was warmed to -30°C and stirred at this temperature for 30 min, and then a solution of compound 1 (2.16 g, 6.0 mmol) in THF (100 mL) was added. The reaction was stirred at room temperature for 3 h and then was quenched with aqueous saturated ammonium chloride (100 mL). After separation, the aqueous phase was extracted with ethyl acetate (EA) (100 mL \times 2). Combined organic layers were evaporated *in vacuo*, and the residue was purified by column chromatography on silica gel, giving compound 3 (2.8 g, 92%) as a white solid, with a melting point (mp) of $73\text{--}75^{\circ}\text{C}$. Because of the existence of two kinetically distinct conformations of compound 3, two sets of nuclear magnetic resonance (NMR) were

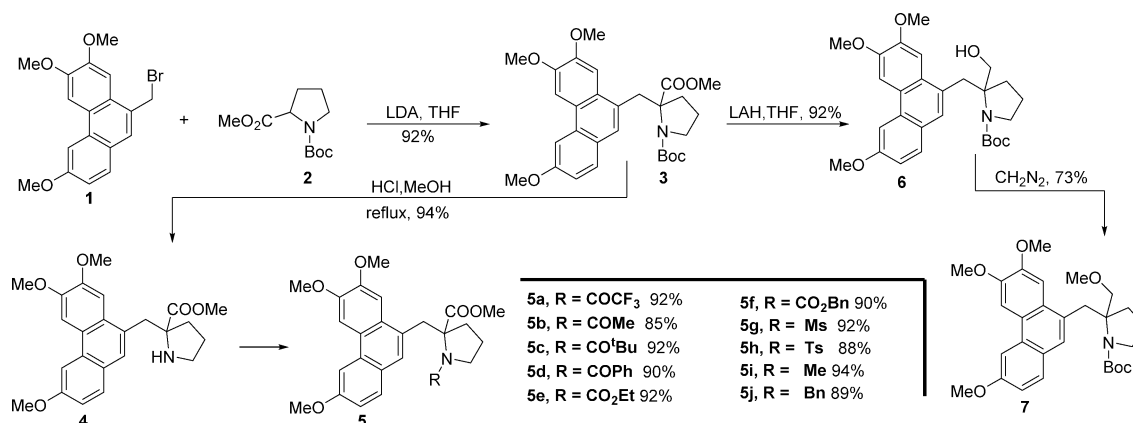


Figure 3. Synthetic route of D-ring opened phenanthroindolizidine alkaloid analogues.

observed. For NMR data, see the [Supporting Information](#). HRMS calcd for $C_{29}H_{35}NO_7$ ($M + Na$)⁺, 532.2306; found, 532.2310.

Methyl-2-((3,6,7-trimethoxyphenanthren-9-yl)methyl)pyrrolidine-2-carboxylate (4). To a solution of compound 3 (4.0 g, 7.86 mmol) in MeOH (200 mL) was added aqueous HCl (12 M, 3 mL). The reaction was heated at reflux for 2 h, and then the solvent was evaporated *in vacuo*. To the residue was added water (200 mL) and aqueous NaOH to pH 14, and the resulting solution was extracted with DCM (80 mL × 3). Combined organic layers were washed with brine, dried over Na_2SO_4 , filtered, and evaporated to give compound 4 (3.2 g, 94%) as a white solid, with a mp of 162–163 °C. For NMR data, see the [Supporting Information](#). HRMS [matrix-assisted laser desorption/ionization (MALDI)] m/z calcd for $C_{24}H_{28}NO_5$ ($M + H$)⁺, 410.1962; found, 410.1965.

Methyl-1-(2,2,2-trifluoroacetyl)-2-((3,6,7-trimethoxyphenanthren-9-yl)methyl)pyrrolidine-2-carboxylate (5a). To a solution of compound 4 (0.41 g, 1.0 mmol) and 4-dimethylaminopyrrolidine (DMAP) (0.15 g, 1.2 mmol) in DCM (40 mL) was added a solution of trifluoroacetic anhydride (TFAA) (0.20 g, 1.1 mmol) in DCM (10 mL) dropwise at room temperature. After 2 h, the reaction mixture was washed with diluted aqueous HCl, water, and brine. After the solution was dried over Na_2SO_4 , it was evaporated and the resulting residue was purified by column chromatography on silica gel to give compound 5a (0.46 g, 92%) as a white solid, with a mp of 174–175 °C. For NMR data, see the [Supporting Information](#). HRMS (MALDI) m/z calcd for $C_{26}H_{26}F_3NO_6Na$ ($M + Na$)⁺, 528.1604; found, 528.1603.

Methyl-1-acetyl-2-((3,6,7-trimethoxyphenanthren-9-yl)methyl)pyrrolidine-2-carboxylate (5b). Compound 5b was obtained using a synthetic procedure similar to that of compound 5a as a white solid (85%), with a mp of 208–210 °C. For NMR data, see the [Supporting Information](#). HRMS (MALDI) m/z calcd for $C_{26}H_{29}NO_6Na$ ($M + Na$)⁺, 474.1887; found, 474.1895.

Methyl-1-pivaloyl-2-((3,6,7-trimethoxyphenanthren-9-yl)methyl)pyrrolidine-2-carboxylate (5c). Compound 5c was obtained using a synthetic procedure similar to that of compound 5a as a white solid (92%), with a mp of 188–189 °C. For NMR data, see the [Supporting Information](#). HRMS (MALDI) m/z calcd for $C_{29}H_{35}NO_6Na$ ($M + Na$)⁺, 516.2357; found, 516.2350.

Methyl-1-benzoyl-2-((3,6,7-trimethoxyphenanthren-9-yl)methyl)pyrrolidine-2-carboxylate (5d). Compound 5d was obtained using a synthetic procedure similar to that of compound 5a as a white solid (90%), with a mp of 204–206 °C. For NMR data, see the [Supporting Information](#). HRMS (MALDI) m/z calcd for $C_{31}H_{33}NO_6Na$ ($M + Na$)⁺, 536.2044; found, 536.2042.

1-Ethyl-2-methyl-2-((3,6,7-trimethoxyphenanthren-9-yl)methyl)pyrrolidine-1,2-dicarboxylate (5e). Compound 5e was obtained using a synthetic procedure similar to that of compound 5a as a white solid (92%), with a mp of 129–131 °C. For NMR data, see the [Supporting Information](#). HRMS (MALDI) m/z calcd for $C_{27}H_{31}NO_7Na$ ($M + Na$)⁺, 504.1993; found, 504.1996.

1-Benzyl-2-methyl-2-((3,6,7-trimethoxyphenanthren-9-yl)methyl)pyrrolidine-1,2-dicarboxylate (5f). Compound 5f was obtained using a synthetic procedure similar to that of compound 5a as a white solid (90%), with a mp of 153–155 °C. For NMR data, see the [Supporting Information](#). HRMS (MALDI) m/z calcd for $C_{32}H_{33}NO_7Na$ ($M + Na$)⁺, 566.2149; found, 566.2149.

Methyl-1-(methylsulfonyl)-2-((3,6,7-trimethoxyphenanthren-9-yl)methyl)pyrrolidine-2-carboxylate (5g). Compound 5g was obtained using a synthetic procedure similar to that of compound 5a as a white solid (88%), with a mp of 169–171 °C. For NMR data, see the [Supporting Information](#). HRMS (MALDI) m/z calcd for $C_{25}H_{29}NO_7SNa$ ($M + Na$)⁺, 510.1557; found, 510.1555.

Methyl-1-tosyl-2-((3,6,7-trimethoxyphenanthren-9-yl)methyl)pyrrolidine-2-carboxylate (5h). Compound 5h was obtained using a synthetic procedure similar to that of compound 5a as a white solid (88%), with a mp of 205–206 °C. For NMR data, see the [Supporting Information](#). HRMS (MALDI) m/z calcd for $C_{31}H_{33}NO_7SNa$ ($M + Na$)⁺, 586.1870; found, 586.1863.

Methyl-1-methyl-2-((3,6,7-trimethoxyphenanthren-9-yl)methyl)pyrrolidine-2-carboxylate (5i). To a solution of compound 4 (0.37 g, 0.91 mmol) and aqueous formic aldehyde (30%, 0.15 mL) in MeOH (40 mL) was added $NaBH_3CN$ (0.12 g, 1.9 mmol). The reaction was stirred at room temperature for 4 h and then quenched with saturated aqueous ammonium chloride (50 mL). The solution was extracted with DCM (30 mL × 3), and the combined organic layers were washed with brine, dried over Na_2SO_4 , filtered, and evaporated. The resulting residue was purified by column chromatography on silica gel to give compound 5i (0.37 g, 94%) as a white solid, with a mp of 108–110 °C. For NMR data, see the [Supporting Information](#). HRMS (MALDI) m/z calcd for $C_{25}H_{29}NO_5Na$ ($M + Na$)⁺, 446.1937; found, 446.1941.

Methyl-1-benzyl-2-((3,6,7-trimethoxyphenanthren-9-yl)methyl)pyrrolidine-2-carboxylate (5j). Compound 5j was obtained using a synthetic procedure similar to that of compound 5i as a white solid (89%), with a mp of 110–112 °C. For NMR data, see the [Supporting Information](#). HRMS (MALDI) m/z calcd for $C_{31}H_{33}NO_5Na$ ($M + Na$)⁺, 522.2251; found, 522.2256.

tert-Butyl-2-(hydroxymethyl)-2-((3,6,7-trimethoxyphenanthren-9-yl)methyl)pyrrolidine-1-carboxylate (6). To a suspension of $LiAlH_4$ (85 mg, 2.2 mmol) in THF (100 mL) at -78 °C was added compound 3 (0.94 g, 1.85 mmol) in one portion. The reaction was stirred at -20 °C for 2 h and then quenched with saturated aqueous ammonium chloride. The solvent was evaporated *in vacuo*, and the resulting residue was dissolved in DCM, which was washed with water and brine. After the solution was dried over Na_2SO_4 , filtered, and evaporated, the resulting residue was purified by column chromatography on silica gel to give compound 6 (0.81 g, 92%), with a mp of 178–180 °C. For NMR data, see the [Supporting Information](#). HRMS (MALDI) m/z calcd for $C_{28}H_{35}NO_6Na$ ($M + Na$)⁺, 504.2357; found, 504.2359.

tert-Butyl-2-(methoxymethyl)-2-((3,6,7-trimethoxyphenanthren-9-yl)methyl)pyrrolidine-1-carboxylate (7). To a sol-

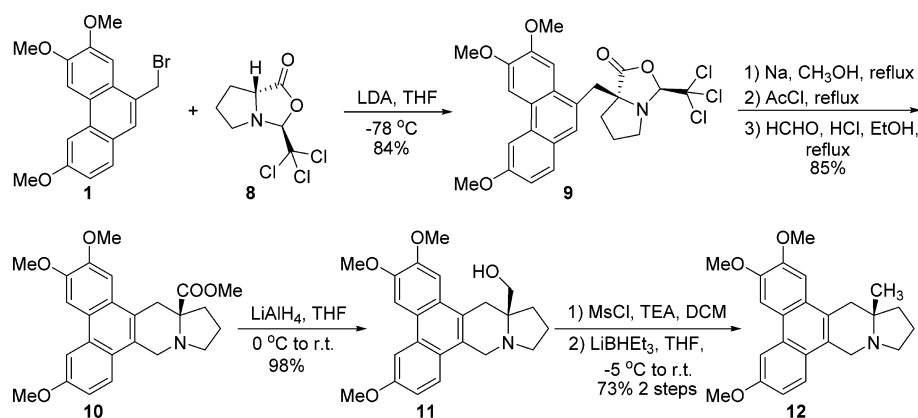


Figure 4. Enantioselective synthetic route of 13a-substituted phenanthroindolizidine alkaloid analogues.

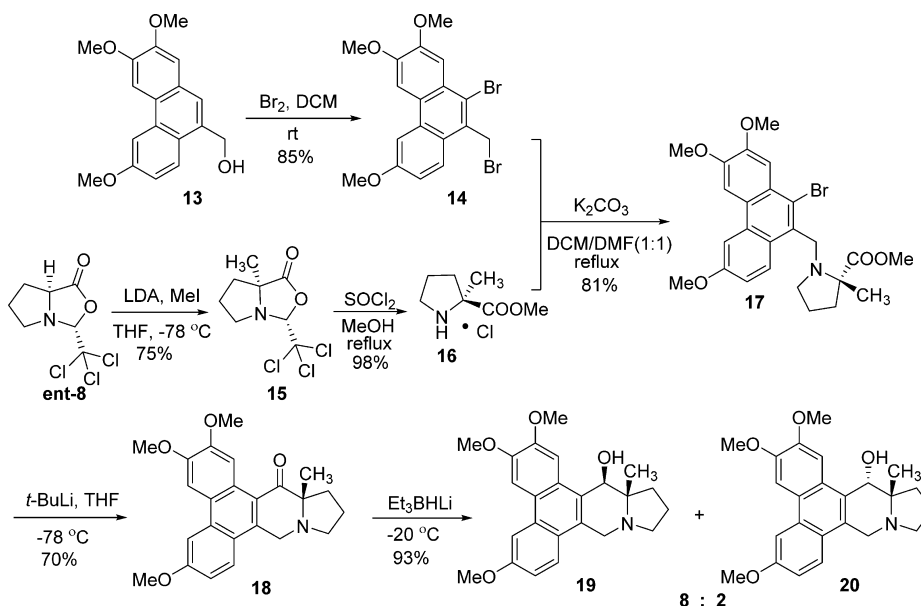


Figure 5. Enantioselective synthetic route of optical 13a-methyl-14-substituted phenanthroindolizidine alkaloid analogues.

ution of compound **6** (0.47 g, 0.98 mmol) and $\text{BF}_3 \cdot \text{Et}_2\text{O}$ (0.01 mL) in DCM (20 mL) was added a solution of CH_2N_2 in ether until the starting material was consumed completely, which was monitored by thin-layer chromatography (TLC). After the reaction was completed, the reaction was quenched with acetic acid. The reaction mixture was then washed with water and brine, dried over Na_2SO_4 , filtered, and evaporated, and the resulting residue was purified by column chromatography on silica gel to give compound **7** (0.36 g, 73%), with a mp of 129–130 °C. For NMR data, see the [Supporting Information](#). HRMS (MALDI) m/z calcd for $\text{C}_{29}\text{H}_{37}\text{NO}_6\text{Na}$ ($M + \text{Na}$)⁺, 518.2513; found, 518.2507.

The other compounds used for the bioassay were prepared according to our recently developed synthetic methods.^{31,32}

Antiviral Biological Assay.²⁴ The bioassays of *in vitro* and *in vivo* anti-TMV activity were carried out on *Nicotiana tabacum* L. The upper leaves of *N. tabacum* L. were first inoculated with TMV, then were selected and ground in phosphate buffer, and then filtered through double-layer pledget. The filtrate was centrifuged, treated with polyethylene glycol (PEG) twice, and then centrifuged again. The whole experiment was processed at 4 °C. The main difference of three *in vivo* modes was as follows: For protective effects, the leaves were first treated with a solution of specific compound and then were inoculated with TMV. For the inactivation effect, the leaf was directly inoculated with TMV that has been treated with a solution of specific compound. For the curative effect, the leaves were first inoculated with TMV and then treated with a solution of specific compound.

RESULTS AND DISCUSSION

Chemistry. As shown in [Figure 3](#), the synthesis of the D-ring opened phenanthroindolizidine alkaloid analogues commenced with the coupling of two known compounds, phenanthryl bromide **1** and proline derivative **2**,³³ giving compound **3** in 92% yield. Under acidic conditions, the protecting group (Boc) of compound **3** was easily removed, resulting in amine **4** in 94% yield. Compounds **5a–5j** were readily prepared from compound **4** via corresponding acylation, sulfonylation, and alkylation reactions. Treatment of compound **3** with LiAlH_4 gave reduced compound **6**, which was then methylated using diazomethane as a methylation reagent. The enantioselective synthesis of 13a-substituted phenanthroindolizidine alkaloid analogues was shown in [Figure 4](#).³¹ Using phenanthryl bromide **1** and optical oxazolidinone **8** as starting material, enantiopure compound **9** could be obtained as a single diastereoisomer in good yield. Compound **9** was then transformed to 13a-methylcarboxylate phenanthroindolizidine **10** via a sequential base-promoted ring opening of oxazolidinone, followed by acid-promoted deprotection of the 2,2-disubstituted proline derivative and Pictet–Spengler cyclization. Ester **10** was reduced by LiAlH_4 in a nearly quantitative yield to give alcohol **11**. After extensive screening

of reaction conditions, the hydroxyl group of alcohol **11** could be transformed to methyl, giving 13a-methyl antofine analogue **12** via a methanesulfonylation and superhydride reduction consequence. Enantiopure 13a-methyl-14-substituted antofine analogues were prepared as shown in Figure 5.³² From the treatment of the readily available phenanthryl alcohol **13** with bromine in DCM at room temperature, dibromide compound **14** was obtained in 85% yield. The other part **16** needed for the following alkylation was prepared from optical oxazolidinone **ent-8** through modified Seebach's self-regeneration of stereocenters (SRS) strategy to introduce a methyl group, which was followed by acid-promoted methylation and deprotection sequences. The following coupling of compound **17** and dibromide **14** was not so seemingly easy, because compound **16** was hygroscopic and dibromide **14** was liable to moisture. After extensive screening of reaction conditions, including bases, solvents, and reaction temperatures, the desired product **17** could be obtained in good yield when K_2CO_3 (5 equiv) was employed as a base in refluxed mixed solvents (1:1 DCM/DMF). Then, the key intermediate **17** was transformed to pentacyclic compound **18** through the Parham cycloacylation reaction. To achieve stereoselective reduction of ketone **18**, a variety of hydride reagents were examined. It was found that when superhydride ($LiEt_3BH$) was used as the reducing agent, the best selectivity (8:2 **19/20**) was obtained. Using less steric $LiAlH_4$ as a hydride source, the opposite selectivity was observed.

To judge the antiviral potency of the synthesized D-ring opened phenanthrolizidine analogues **3**, **4**, **5a–5j**, **6**, and **7** and chiral 13a- and/or 14-substituted phenanthroindolizidines (**10–12**, **18–20**, **ent-10–ent-12**, and **ent-18–ent-20**), ribavirin and Ningnanmycin, two successful commercial plant virucides, were selected as the controls. To further investigate the influence of the substitutions at the 13a position and in-depth SARs under the chiral scenario, enantiopure 13a-H phenanthroindolizidines (*S*)-antofine, (*R*)-antofine, and racemic 13-methyl antofine were also used for comparison, which were prepared by our previously reported methods.²⁶ The *in vitro* and *in vivo* (under three models: protection, inactivation, and curative effect) activities against TMV of phenanthroindolizidine alkaloid analogues, ribavirin, and Ningnanmycin were shown in Table 1.

The *in vitro* anti-TMV bioassay showed that most of the synthesized compounds except for compounds **6** and **10** exhibited higher or comparable anti-TMV activity compared to ribavirin at both high ($500 \mu\text{g mL}^{-1}$) and low ($100 \mu\text{g mL}^{-1}$) concentrations. Importantly, almost half of the compounds (e.g., **4**, **5j**, **11**, **19**, **20**, **ent-10**, **ent-11**, **ent-12**, and **ent-20**) exhibited a similar inhibitory effect against TMV with Ningnanmycin, perhaps the most effective commercial plant virucide. Because most of the synthesized antofine analogues displayed distinguished *in vitro* antiviral activity against TMV, further investigations of their antiviral activity *in vivo* were deserved. Then, *in vivo* activities were assayed in three models (protection, deactivation, and curative) (Table 1).

Further *in vivo* anti-TMV activities showed that these new synthesized phenanthroindolizidine alkaloid analogues displayed a good to excellent inhibitory effect, which, in general, exhibited the same trend to the *in vitro* activities. Especially, compound **ent-11** showed a much more potent inhibitory effect against TMV than the most effective commercial virucide Ningnanmycin. Interestingly, although compounds **11**, **19**, **20**, **ent-10**, **ent-12**, and **ent-20** exhibited inferior activity at $500 \mu\text{g mL}^{-1}$

Table 1. *In Vitro* and *in Vivo* Anti-TMV Activity of Synthesized Compounds

Compd	Conc. ($\mu\text{g/mL}$)	Inhibition rate (%)			
		<i>In Vitro</i> effect	Protection effect	Inactivation effect	Curative effect
3	500	33.3	36.3	37.4	35.8
	100	16.8	9.5	12.3	11.1
4	500	62.5	58.3	56.2	61
	100	25.0	30.2	28.4	26.1
5a	500	42.5	52.0	46.3	54.2
	100	15.3	13.6	20.0	19.0
5b	500	36.1	43.6	39.8	41.1
	100	16.0	17.2	8.3	12.4
5c	500	48.3	44.4	41.4	46.2
	100	19.5	15.1	16.9	16.3
5d	500	50.0	53.1	47.8	49.6
	100	26.2	23.7	13.9	16.8
5e	500	46.2	40.0	43.7	46.5
	100	23.1	13.5	22.1	19.7
5f	500	47.1	42.5	42.0	48.3
	100	25.0	12.3	18.5	18.0
5g	500	44.8	38.7	36.5	41.4
	100	21.7	10.0	15.8	11.0
5h	500	41.8	45.2	46.8	43.2
	100	20.2	23.2	21.7	20.5
5i	500	34.3	40.0	37.8	42.6
	100	13.6	17.1	17.8	23.8
5j	500	60.0	56.8	54.8	58.3
	100	26.3	30.5	28.1	26.1
6	500	31.2	33.4	35.7	39.0
	100	0	0	0	7.6
7	500	46.3	46.1	44.0	43.7
	100	20.4	24.8	25.8	21.4
10	500	32.4	40.0	34.7	35.3
	100	0	10.3	0	0
11	500	58.9	55.2	56.3	54.8
	100	25.0	23.6	20.0	21.4
12	500	40.0	48.3	42.1	45.0
	100	19.7	18.4	15.8	16.9
18	500	42.4	41.6	46.7	44.4
	100	18.6	15.8	15.1	20.0
19	500	61.4	55.8	58.3	57.2
	100	37.6	30.0	32.6	30.3
20	500	54.3	59.3	55.7	60.4
	100	35.9	36.3	30.0	33.0
ent-10	500	53.8	60.0	55.4	58.7
	100	26.2	23.5	22.6	18.2
ent-11	500	85.3	78.1	80.1	88.4
	100	52.5	48.3	58.4	67.8
ent-12	500	55.5	59.4	57.8	49.2
	100	24.0	30.9	28.2	21.5
ent-18	500	40.6	39.1	37.0	42.5
	100	22.2	17.1	14.2	19.3
ent-19	500	53.0	53.2	47.5	45.8
	100	26.7	21.5	20.0	17.3
ent-20	500	63.8	65.2	62.4	55.7
	100	33.3	42.6	38.5	28.6
(S)-antofine	500	60.2	51.1	55.5	56.4
	100	30.5	37.2	26.7	28.4
(R)-antofine	500	65.8	55.7	58.0	62.5
	100	30.4	32.3	29.4	33.4
13a-Me-antofine	500	47.1	45.4	41.3	43.6
	100	22.4	29.8	17.5	23.7
Ribavirin	500	41.3	38.9	37.2	39.4
	100	18.5	15.6	11.9	14.7
Ningnanmycin	500	69.3	57.9	54.2	58.7
	100	26.8	38.4	20.0	23.1

mL^{-1} compared to Ningnanmycin, they showed higher or comparable inhibitory effect at $100 \mu\text{g mL}^{-1}$. In other words, these compounds could still keep very potent antiviral activities even at a low concentration. Although most of the other compounds showed less potent inhibitory effects than

Ningnanmycin, they displayed better or at least comparable activities than the other popular virucide ribavirin that was used as a control.

SARs demonstrated that, although, as the controls, the naturally occurring 13a-H phenanthrylindolizidine alkaloid (*R*)-antofine showed comparable antiviral activities at both high and low concentrations with its unnatural antipode (*S*)-antofine, all of the synthesized 13a-substituted phenanthrylindolizidine analogues **ent-10**, **ent-11**, and **ent-12** exhibited more potent antiviral effect than their corresponding configurationally enantiomers **10**, **11**, and **12**, respectively. These interesting results obviously demonstrated that spatial configuration of the molecules was very crucial for keeping high bioactivities and introduction of suitable functional groups at the 13a position could accelerate this trend. Both compounds **18** and **ent-18** possessing a ketone group on the six-membered D ring, which makes the D ring of the molecules more planar and, thus, increases the molecular rigidity, were less effective than compounds **12** and **ent-12**. After reduction of the ketones **18** and **ent-18**, the high rigidity of the molecule was released to some extent and the resulting 13a-methyl-14-hydroxyl phenanthroindolizidine analogues (**19**, **20**, **ent-19**, and **ent-20**) displayed higher inhibitory effect against TMV. However, more interestingly, most of the D-ring opened analogues, which became more flexible spatially, could also show comparable or even higher (**5a** and **5j**) anti-TMV activities than 13a-methyl antofine. These results indicated that 3D conformation of phenanthroindolizidine analogues was also an important factor that can influence bioactivities. Another interesting observation was that the hydroxyl group at either the 13a or 14 position was helpful for keeping high biological activities; for example, compounds **11**, **19**, **20**, **ent-11**, **ent-19**, and **ent-20** showed more effective or at least a comparable inhibitory effect compared to the 13a-methyl analogues **12** and **ent-12**, which may suggest that a hydrogen-donating hydroxyl group at this domain was favorable.

In summary, to explore the influence of spatial configuration and 3D conformation of phenanthroindolizidine alkaloid analogues on the activities, a series of D-ring opened phenanthroindolizidine alkaloid analogues and chiral 13a- and/or 14-substituted analogues were synthesized and evaluated for their antiviral activities against TMV. The bioassay results indicated that most of the chiral phenanthroindolizidine analogues showed good to excellent *in vivo* anti-TMV activity, among which compound **11** displayed a more potent inhibitory effect than Ningnanmycin, thus emerging as a potential inhibitor of the plant virus. An in-depth SAR investigation showed that substitution patterns at 13a and/or 14 positions have a great effect on the anti-TMV activity, demonstrating that spatial configuration is of importance for keeping high activity. Molecular planarity and rigidity of the D ring also greatly influence activity, showing that 3D conformation is also very crucial for improving bioactivity. Then, it is noteworthy that a hydrogen donor at the 13a or 14 position may be another essential factor for antiviral investigation. Further investigations on structural optimization and mode of action are currently underway in our laboratories.

■ ASSOCIATED CONTENT

■ Supporting Information

The Supporting Information is available free of charge on the ACS Publications website at DOI: 10.1021/acs.jafc.5b06112.

Detailed synthetic procedure (PDF)

■ AUTHOR INFORMATION

Corresponding Author

*Telephone/Fax: +86-022-23503952. E-mail: wangqm@nankai.edu.cn.

Funding

The authors are grateful to the National Natural Science Foundation of China (21132003, 21421062, and 21372131) and the Specialized Research Fund for the Doctoral Program of Higher Education (20130031110017) for generous financial support for their research programs.

Notes

The authors declare no competing financial interest.

■ REFERENCES

- (1) Scholthof, K.-B. G. TOBACCO MOSAIC VIRUS: A Model System for Plant Biology. *Annu. Rev. Phytopathol.* **2004**, *42*, 13–34.
- (2) Hari, V.; Das, P. Ultra microscopic detection of plant viruses and their gene products. In *Plant Disease Virus Control*; Hadidi, A., Khetarpal, R. K., Koganezawa, H., Eds.; APS Press: St. Paul, MN, 1998; pp 417–427.
- (3) Bos, L. 100 years of virology: from vitalism via molecular biology to genetic engineering. *Trends Microbiol.* **2000**, *8*, 82–87.
- (4) Ouyang, G. P.; Cai, X. J.; Chen, Z.; Song, B. A.; Bhadury, P. S.; Yang, S.; Jin, L. H.; Xue, W.; Hu, D. Y.; Zeng, S. Synthesis and antiviral activities of pyrazole derivatives containing an oxime moiety. *J. Agric. Food Chem.* **2008**, *56*, 10160–10167.
- (5) Reichman, M.; Devash, Y.; Suhadolnik, R. J.; Sela, I. Human leukocyte interferon and the antiviral factor (AVF) from virus-infected plants stimulate plant tissues to produce nucleotides with antiviral activity. *Virology* **1983**, *128*, 240–244.
- (6) Chen, M. H.; Chen, Z.; Song, B. A.; Bhadury, P. S.; Yang, S.; Cai, X. J.; Hu, D. Y.; Xue, W.; Zeng, S. Synthesis and antiviral activities of chiral thiourea derivatives containing an α -aminophosphonate moiety. *J. Agric. Food Chem.* **2009**, *57*, 1383–1388.
- (7) Li, Y. M.; Zhang, Z. K.; Jia, Y. T.; Shen, Y. M.; He, H. P.; Fang, R. X.; Chen, X. Y.; Hao, X. J. 3-Acetyl-3-hydroxyindole: A new inducer of systemic acquired resistance in plants. *Plant Biotechnol. J.* **2008**, *6*, 301–308.
- (8) Sidwell, R. W.; Huffman, J. H.; Khare, G. P.; Allen, L. B.; Witkowski, J. T.; Robins, R. K. Broad-spectrum antiviral activity of virazole: 1- β -D-Ribofuranosyl-1,2,4-triazole-3-carboxamide. *Science* **1972**, *177*, 705–706.
- (9) Bachrach, U. Antiviral activity of oxidized polyamines. *Amino Acids* **2007**, *33*, 267–272.
- (10) De Meester, C. Genotoxic potential of β -carbolines: A review. *Mutat. Res., Rev. Genet. Toxicol.* **1995**, *339*, 139–153.
- (11) Qian, X. H.; Lee, P. W.; Cao, S. China: forward to the green pesticides via a basic research program. *J. Agric. Food Chem.* **2010**, *58*, 2613–2623.
- (12) Seiber, J. N. Sustainability and agricultural and food chemistry. *J. Agric. Food Chem.* **2011**, *59*, 1–2.
- (13) Gellert, E. The indolizidine alkaloids. *J. Nat. Prod.* **1982**, *45*, 50–73.
- (14) Gellert, E.; Rudzats, R. The antileukemia activity of tylocrebrine. *J. Med. Chem.* **1964**, *7*, 361–362.
- (15) Damu, A. G.; Kuo, P. C.; Shi, L. S.; Li, C. Y.; Kuoh, C. S.; Wu, P. L.; Wu, T. S. Phenanthroindolizidine alkaloids from the stems of *Ficus septica*. *J. Nat. Prod.* **2005**, *68*, 1071–1075.
- (16) Yang, C. W.; Chen, W. L.; Wu, P. L.; Tseng, H. Y.; Lee, S. J. Antiinflammatory mechanisms of phenanthroindolizidine alkaloids. *Mol. Pharmacol.* **2006**, *69*, 749–758.
- (17) Baumgartner, B.; Erdelmeier, C. A. J.; Wright, A. D.; Rali, T.; Sticher, O. An antimicrobial alkaloid from *Ficus septica*. *Phytochemistry* **1990**, *29*, 3327–3330.

- (18) Choi, J. Y.; Gao, W.; Odegard, J.; Shiah, H. S.; Kashgarian, M.; McNiff, J. M.; Baker, D. C.; Cheng, Y. C.; Craft, J. Abrogation of skin disease in LUPUS-prone MRL/FASlpr mice by means of a novel tylophorine analog. *Arthritis Rheum.* **2006**, *54*, 3277–3283.
- (19) An, T. Y.; Huang, R. Q.; Yang, Z.; Zhang, D. K.; Li, G. R.; Yao, Y. C.; Gao, J. Alkaloids from *Cyanachum komarovii* with inhibitory activity against the tobacco mosaic virus. *Phytochemistry* **2001**, *58*, 1267–1269.
- (20) Xi, Z.; Zhang, R. Y.; Yu, Z. H.; Ouyang, D. The interaction between tylophorine B and TMV RNA. *Bioorg. Med. Chem. Lett.* **2006**, *16*, 4300–4304.
- (21) Pettit, G. R.; Goswami, A.; Cragg, G. M.; Schmidt, J. M.; Zou, J.-C. Antineoplastic Agents, 103. The Isolation and Structure of Hypoestestatin 1 and 2 From the East African *Hypoestes verticillaris*. *J. Nat. Prod.* **1984**, *47*, 913–919.
- (22) Ali, M.; Bhutani, K. K. Minor Alkaloids of *Tylophora hirsuta*. *Phytochemistry* **1987**, *26*, 2089–2092.
- (23) Ali, M.; Bhutani, K. K. Alkaloids From *Tylophora indica*. *Phytochemistry* **1989**, *28*, 3513–3517.
- (24) Wang, K.; Su, B.; Wang, Z.; Wu, M.; Li, Z.; Hu, Y.; Fan, Z.; Mi, N.; Wang, Q. Synthesis and Antiviral Activities of Phenanthroindolizidine Alkaloids and Their Derivatives. *J. Agric. Food Chem.* **2010**, *58*, 2703–2709.
- (25) Wang, Z.; Wei, P.; Xizhi, X.; Liu, Y.; Wang, L.; Wang, Q. Design, Synthesis, and Antiviral Activity Evaluation of Phenanthrene-Based Antofine Derivatives. *J. Agric. Food Chem.* **2012**, *60*, 8544–8551.
- (26) Wang, Z.; Wei, P.; Wang, L.; Wang, Q. Design, Synthesis, and Anti-tobacco Mosaic Virus (TMV) Activity of Phenanthroindolizidines and Their Analogues. *J. Agric. Food Chem.* **2012**, *60*, 10212–10219.
- (27) Wang, Z.; Wang, L.; Ma, S.; Liu, Y.; Wang, L.; Wang, Q. Design, Synthesis, Antiviral Activity, and SARs of 14-Aminophenanthroindolizidines. *J. Agric. Food Chem.* **2012**, *60*, 5825–5831.
- (28) Wu, M.; Han, G.; Wang, Z.; Liu, Y.; Wang, Q. Synthesis and Antiviral Activities of Antofine Analogues with Different C-6 Substituent Groups. *J. Agric. Food Chem.* **2013**, *61*, 1030–1035.
- (29) Su, B.; Chen, F.; Wang, L.; Wang, Q. Design, Synthesis, Antiviral Activity, and Structure–Activity Relationships (SARs) of Two Types of Structurally Novel Phenanthroindo/quinolizidine Analogues. *J. Agric. Food Chem.* **2014**, *62*, 1233–1239.
- (30) Su, B.; Cai, C.; Deng, M.; Liang, D.; Wang, L.; Wang, Q. Design, synthesis, antiviral activity, and SARs of 13a-substituted phenanthroindolizidine alkaloid derivatives. *Bioorg. Med. Chem. Lett.* **2014**, *24*, 2881–2884.
- (31) Su, B.; Cai, C.; Wang, Q. Enantioselective Approach to 13a-Methylphenanthroindolizidine Alkaloids. *J. Org. Chem.* **2012**, *77*, 7981–7987.
- (32) Su, B.; Deng, M.; Wang, Q. The First Enantioselective Approach to 13a-Methyl-14-hydroxyphenanthroindolizidine Alkaloids—Synthetic Studies towards Hypoestestatin 2. *Eur. J. Org. Chem.* **2013**, *2013*, 1979–1985.
- (33) Su, B.; Cai, C. L.; Deng, M.; Liang, D. M.; Wang, L. Z.; Wang, Q. M. Design, synthesis, antiviral activity, and SARs of 13a-substituted phenanthroindolizidine alkaloid derivatives. *Bioorg. Med. Chem. Lett.* **2014**, *24*, 2881–2884.